Journal of Anatomy

J. Anat. (2011) **219**, pp490–501 doi: 10.1111/j.1469-7580.2011.01399.x

Sustained swimming increases the mineral content and osteocyte density of salmon vertebral bone

Geir K. Totland,[1] Per Gunnar Fjelldal,[2] Harald Kryvi,[1] Guro Løkka,[1] Anna Wargelius,[2] Anita Sagstad,[1] Tom Hansen[2] and Sindre Grotmol[1]

[1]*Department of Biology, University of Bergen, Bergen, Norway*
[2]*Department of Aquaculture, Institute of Marine Research (IMR), Matre Aquaculture Research Station, Matredal, Norway*

Abstract

This study addresses the effects of increased mechanical load on the vertebral bone of post-smolt Atlantic salmon by forcing them to swim at controlled speeds. The fish swam continuously in four circular tanks for 9 weeks, two groups at 0.47 body lengths (bl) $\times$ s^{-1} (non-exercised group) and two groups at 2 bl $\times$ s^{-1} (exercised group), which is just below the limit for maximum sustained swimming speed in this species. Qualitative data concerning the vertebral structure were obtained from histology and electron microscopy, and quantitative data were based on histomorphometry, high-resolution X-ray micro-computed tomography images and analysis of bone mineral content, while the mechanical properties were tested by compression. Our key findings are that the bone matrix secreted during sustained swimming had significantly higher mineral content and mechanical strength, while no effect was detected on bone *in vivo* architecture. mRNA levels for two mineralization-related genes *bgp* and *alp* were significantly upregulated in the exercised fish, indicating promotion of mineralization. The osteocyte density of the lamellar bone of the amphicoel was also significantly higher in the exercised than non-exercised fish, while the osteocyte density in the cancellous bone was similar in the two groups. The vertebral osteocytes did not form a functional syncytium, which shows that salmon vertebral bone responds to mechanical loading in the absence of an extensive connecting syncytial network of osteocytic cell processes as found in mammals, indicating the existence of a different mechanosensing mechanism. The adaptive response to increased load is thus probably mediated by osteoblasts or bone lining cells, a system in which signal detection and response may be co-located. This study offers new insight into the teleost bone biology, and may have implications for maintaining acceptable welfare for farmed salmon.

Key words: *alp*; Atlantic salmon; *bgp*; bone mineral content; mechanical load; osteocyte density; stiffness; vertebra.

Introduction

Bones contribute to locomotion by offering a complex system of rigid levers that, in conjunction with muscles, have played a key role in the development of refined modes of vertebrate movement. When vertebrates became land-dwellers, their skeleton gradually developed the ability to bear weight. The most important characteristics of bone lie in its structural and mechanical properties. Bone tissue is initially secreted by osteoblasts as non-mineralized osteoid. During osteogenesis, osteoblasts may loose polarity and become entombed in the extracellular matrix in the form of osteocytes. The solid extracellular matrix consists of an organic and a mineral phase. The organic phase is primarily made up of type I collagen fibres that provide toughness and viscoelasticity, while the mineral phase consists of hydroxyapatite crystals that enable the bone to withstand various forms of stress generated through movement and, on land, its dealings with gravity.

Generally speaking, at anatomical sites of high strain energy, bone formation is stimulated and resorption suppressed in mammals, resulting in a local increase in bone mass (Currey, 1984, 2003; Carter et al. 1996; Timlin et al. 2000; Notomi et al. 2001; Huang et al. 2003). Moreover, as has been shown in mice, the quality of the bone matrix, such as the extent of mineral incorporation and the arrangement and density of collagen fibrils, may also contribute to the modulation of its mechanical integrity (Burr, 2002; Turner & Robling, 2005; Turner, 2006; Wallace et al. 2007; Turner et al. 2009). Bone resorption is mainly performed by osteoclasts, which thus play a pivotal role in

Correspondence
Geir K. Totland, Department of Biology, University of Bergen, Thormøhlensgate 55, NO-5008 Bergen, Norway. E: geir.totland@bio.uib.no

Accepted for publication *27 Apr 2011*
Article published online *25 May 2011*

the dynamics of bone remodelling, a process that takes place during growth and in the constant tuning of bone to functional requirements, the mechanical load generated through exercise or disuse.

Due to the stringent demands imposed by the density of water, the skeleton of teleost fish such as salmon performs specific functions that differ from those of terrestrial vertebrates. For example, the skeleton does not need to counteract gravity, i.e. bear weight; hence, the main loads on the vertebral column arise from the forces generated by the fish itself, and its primary task is therefore to support axial oscillations of the body and tail during swimming (see review by Wardle et al. 1995). The combined function of the vertebrae, muscle segments and myosepts is to produce a wave of curvature that travels towards the tail while, under lateral flexion of the vertebrae, generating a minimum loss of power in the form of tension, compression and torsion (see review by Liao, 2007). At the same time, the vertebrae are designed to cope with the strains involved in the production of lateral jets of fluid (Fig. 1a,b). The forces exerted along the vertebral column during the propulsory beat-cycle are dependent on the species-specific swimming mode. In salmonids, for example, the tail and tailfin undulate and, to increase thrust, more of the body takes part in this movement. Here, the highest strains are placed in the mid-region of the backbone (Coughlin et al. 2004) where the largest and most highly mineralized vertebrae are found (Fjelldal et al. 2004, 2005, 2006). Correspondingly, long-distance cruisers that inhabit the open sea show a higher vertebral bone mineral content (BMC) than species that live a stationary life near the bottom (Meunier & Ramzu, 2006).

As in mammals, teleost bone may also adapt to use and disuse; the exposure of rainbow trout to different water current strengths throughout their lifecycle affects vertebral mineral content and remodelling (Deschamps et al. 2009). Similarly, the trabecular density of jaw bone may respond to feed texture; cichlids fed snails develop higher-density bone than those that are given soft feed (Huysseune et al. 1994). These observations confirm that there is an inherent ability to respond and adapt; teleosts, like mammals, possess a system for mechanosensing.

In mammals, the osteocytes possess long dendritic processes that run through canaliculi within the bone matrix, forming a network that enables them to communicate with each other (Meunier, 2002; Robling & Turner, 2009; Witten & Huysseune, 2009) and with cells at the bone surface (Palumbo et al. 1990) by means of gap junctions. The functional osteocyte syncytium seems to be ideally suited to act as a mechanosensing apparatus that may detect strain throughout the matrix and transduce the cellular signals to orchestrate osteoblast and osteoclast activity where this is most needed to strengthen bone. The cellular mechanisms that underlie this strain-related process of adaptive bone remodelling have not yet been fully unravelled (Cowin et al. 1991; Mullender & Huiskes, 1995; Currey, 2003; Bonewald, 2005; Bonewald & Johnson, 2008).

Nevertheless, osteocytic bone is not a synapomorphic character in vertebrates. In teleosts, the largest vertebrate clade, some groups possess osteocytes while others lack them, having 'acellular' or anosteocytic bone (Kölliker, 1859; Moss, 1961, 1965; Weiss & Watabe, 1979; Mullender et al. 1996; Witten & Huysseune, 2009). Osteocytic bone is generally regarded as the ancestral trait, while advanced teleosts display the derived character – anosteocytic bone (Parenti, 1986; Lynne & Parenti, 2008). However, there are exceptions to this simple dichotomy. Osteocytes have also been noted in a number of advanced teleosts (Kölliker, 1859; Meunier & Sire, 1981; Zylberberg et al. 1992; Hughes et al. 1994). Adding complexity to teleost osteocytic bone is the heterogeneous morphology and density of osteocytes, which may differ between species, bones and even within a bone (Stéphan, 1900; Moss, 1961; Meunier, 2002). In some bones, it has been reported that the osteocytes form a

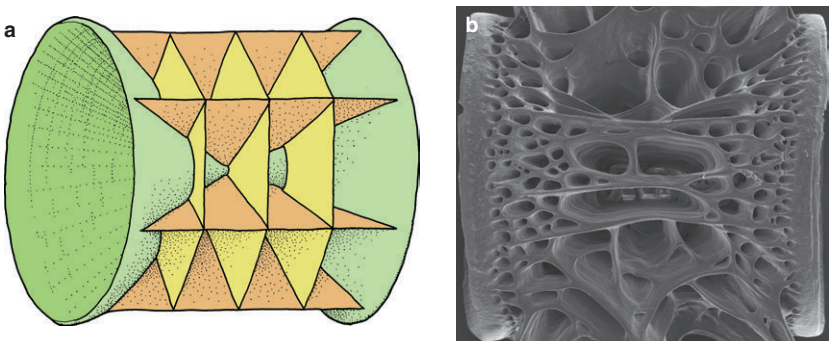

Fig. 1 The amphicoelous architecture of the teleost vertebral body. (a) A generalized schematic illustration. There is no articular surface between the vertebrae; rather, the vertebra pivots on a fluid-filled chamber consisting of notochord tissue. The main growth in length and girth takes place by accretion of bone along the circumferential rims of the cones of the autocentrum (green) and at the distal end of the cancellous interconnected longitudinal (dark orange) and transverse (light orange) bone plates (arcocentrum). (b) Scanning electron microscope of a vertebra showing the spongeous appearance of the cancellous bone.

network of interconnected cell processes (Meunier & Huysseune, 1992; Meunier, 2002), which may function similarly to that of mammals (Huysseune, 2000), while it has been questioned whether the osteocytes in some bones form a functional syncytium (Fiaz et al. 2010).

Whether the teleost bone organs of the locomotor system, such as the vertebrae, respond to the changes in mechanical load in a similar manner to that observed in mammals is an intriguing question. The main aim of this study was to investigate experimentally in salmon how osteocytic bone, bone architecture and mechanical properties may be modulated by an exercise-induced compressive and tensile load generated by the axial musculature during sustained swimming. We also wished to elucidate how genes related to the molecular pathways of bone morphogenesis are expressed. To approach these questions, we performed an exercise experiment on Atlantic salmon post-smolts, which are capable of swimming continuously. An experimental system was constructed that enabled us to tune water velocity, and thus impose mechanical loads within the normal physiological range on the vertebral column.

Materials and methods

Experimental trial

A stock of 77 individually tagged (ID-100A Microtransponder; Trovan, UK) Atlantic salmon post-smolts (weight: $\sim$ 94.5 g; length: $\sim$ 20.7 cm) was X-rayed and screened for deformities, especially of the vertebral column, and all abnormal fish were excluded (n = 9). The remaining fish (n = 68) were randomly allocated to four identical tanks of 17 fish. The tanks employed were circular with the following dimensions: outer diameter 2 m; inner diameter 1.19 m; height 0.5 m; water depth 0.35 m (Fig. 2). A current was generated by water pumped into the tank tangentially along the wall. Current velocities could be adjusted by connecting the pump (EQS4-160/07/A; Flygt, Sundbyberg, Sweden) to a voltage regulator (ACS50; ABB, Helsinki, Finland; Fig. 2), providing an ideal system for studying the influence of chronic exercise by swimming. The water velocity was increased stepwise during a 3-week period in two tanks (exercise group), in order to adapt the fish to coping with increased water velocity through higher swimming speeds, and was kept steady and low in two tanks (non-exercised group), sufficiently fast to clear food particles and faeces. The current speed for the experiment for the non-exercised control group was 0.47 body lengths (bl) $\times$ s^{-1} (13 cm $\times$ s^{-1}), which is close to standard rearing conditions in Norwegian salmon farms, and for the exercised group 1.93 bl $\times$ s^{-1} (52 cm $\times$ s^{-1}), which is just below the limit for maximum sustained swimming speed for Atlantic salmon of this size range (Tang & Wardle, 1992). At this current speed the fish were relatively stationary in water flow. For comparison, wild post-smolt migrate at a mean speed of 1.17 bl $\times$ s^{-1} (Økland et al. 2006). The water exchange rate was kept constant at 15 l $\times$ min^{-1} in all tanks. The water used was 28 ppt seawater with a mean temperature of 11.7 °C. Continuous light was supplied in order to help the fish to orientate themselves and to avoid skin lesions induced by contact with the tank wall at high swimming speed. The fish were fed a commercial diet (Nutra Olympic 3.0 dry feed; Skretting AS, Averøy, Norway) for 1 min every 4 h in excess. The water velocity was maintained during feeding. The experiment was terminated after 9 weeks, and weight and fork length were again recorded. Samples of vertebrae were taken for a range of analyses as described below.

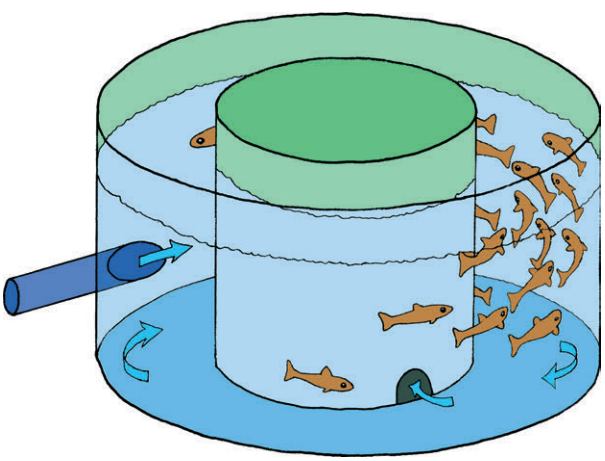

Fig. 2 The experimental tank had a circular channel and current was generated by water injected tangentially into the tank along the inside of the wall. Current velocity was adjusted by a pump voltage regulator.

Sampling

At the termination of the study 12 fish from each tank were X-rayed, while the remaining five fish were used for quantitative polymerase chain reaction (qPCR), histology and micro-computed tomography (micro-CT). The 12 X-rayed fish were further measured for the mechanical properties and mineral content of the vertebral bodies.

Radiography

Lateral radiographs were made using a portable X-ray apparatus (HI-Ray 100; Eickenmeyer Medizintechnik für Tierärzte e.K., Tuttlingen, Germany) and 30 $\times$ 40 cm film (AGFA D4 DW ETE). The film was exposed twice for 50 mA and 72 kV, and developed using a manual developer (Cofar Cemat C56D) with Kodak Professional manual fixer and developer. Images were digitalized by an A3 positive scanner, and the dorso-ventral diameter and length of vertebral bodies were measured by means of image analysis software (IMAGE-PRO PLUS, version 4.0).

Mechanical testing

Vertebrae numbers V40–V43 were tested using a compression jig mounted in a servo-hydraulic machine (TA-XT2; Stable Micro Systems, Godalming, UK). The neural and haemal arches were removed, and the vertebrae were placed between compression plates that were designed in such a way as to remain as close as possible to parallel under load. A compressive load was applied along the cranial–caudal axis, and was adjusted to obtain a constant rate of deformation (0.1 mm s^{-1}). The

resulting load and deformation (mm) were continuously recorded. The resulting load–deformation data were used to calculate the stiffness, yield load and resilience of each vertebra. The calculations were performed using software developed locally. The gradient of the initial near-linear portion of the load–deformation curve is indicative of the structural stiffness of the vertebra along the cranio–caudal axis. The yield load reflects the load that results in deviation from the initial linear (elastic) deformation of the vertebrae, and was defined as the load at the intersection between the load–deformation curve and a 0.2-mm offset line, parallel to the initial linear portion of the curve. The resilience reflects the ability of the vertebra to elastically absorb energy, and is calculated as the area between the load–deformation curve and the *x*-axis, limited by the yield load.

BMC

After mechanical testing, vertebrae V40–V43 were pooled, defatted in hexane baths, dried overnight at 90 °C and then incinerated for 13.5 h in a muffle furnace (115 °C for 0.5 h, 540 °C for 5 h, and 750 °C for 8 h). Each set of vertebrae (V) was weighed individually, and the BMC was expressed as a percentage of mineral weight (MW) per dry weight (DW). The following equation was employed:

$$BMC_{V40-V43} = \frac{MW_{V40-V43}}{DW_{V40-V43}} \times 100$$

Quantification of the three-dimensional vertebral bone structure by X-ray micro-CT

Vertebrae 39–41 were fixed using the same protocol as for histology. The middle vertebra, V40, was analysed, as the likelihood of damage to this vertebrae was low. For stable positioning, each specimen was carefully placed in air in the coned part of a 1.5-mL polypropylene Eppendorf tube. To prevent shrinkage movements during scanning due to drying, a small drop of phosphate-buffered saline (PBS) that did not come into contact with the sample was added to each tube. Scanning was performed in a micro-CT (SkyScan 1072; SkyScan NV, Kontich, Belgium), according to the manufacturer's instructions. The X-ray source was run at 74 kV, and the data sets were acquired with a voxel size of 6.2 μm^3. Stacks of tomographic images were reconstructed from primary shadow images using SKYSCAN software. Three-dimensional digital models of mineralized tissue were constructed from the image stacks by image thresholding and surface rendering, employing IMARIS 4.0.5 software (Bitplane AG, Zürich, Switzerland). In order to compensate for absolute differences in the sizes of vertebrae from different fish, a cylindrical reference volume (VOI) was established for each vertebra (Fig. 3). A range of three-dimensional bone morphometric analyses was performed using a three-dimensional acquisition tool from SkyScan (3D Analyser). The following parameters were evaluated:

1. total bone volume of the vertebral body (TV);
2. percent bone volume (BV/TV) depends on the cylindrical reference volume (VOI);
3. total bone surface (BS) indicates structural complexity and the amount of plates;
4. bone surface/bone volume ratio (BS/BV) also indicates structural complexity and the amount of plates;
5. bone surface density/bone volume signifies the density of surfaces;
6. bone structure thickness;
7. trabecular number indicates the spatial density of bone structures;
8. bone structure separation indicates thickness of empty spaces between bone surfaces;
9. fracture dimension is an index of surface and structural complexity, sensitive to generalized changes in the pattern or spatial scale of structures.

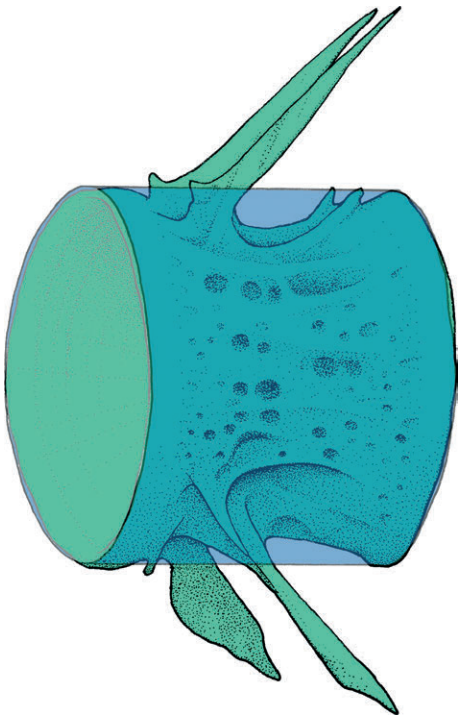

Fig. 3 In order to compensate for absolute differences in sizes of vertebrae from different fish, a cylindrical reference volume (VOI) was established for each vertebra.

Histology and histomorphometry

For histological sections and specimens for grinding, whole vertebrae (V42–44) were fixed by immersion in a solution composed of 10 mL 10% formaldehyde, 10 mL 25% glutaraldehyde, 20 mL 0.2 M cacodylate buffer and 60 mL PBS, whose pH had been adjusted to 7.35. Decalcification was performed in buffered formic acid. V42 was treated in four different ways in order to elucidate details in osteocyte cell shape. (i) Some specimens were rinsed in PBS and dehydrated in ethanol (50, 70 and 96%), before embedding in Technovit 7100 (Heraeus Kulzer GmbH, Hanau, Germany), and semi-thin sections, 1 μm in thickness, were stained with toluidine. As reference species, vertebrae from a bichir (*Polypterus ornatipinnis*) were processed by the same procedure in parallel with the salmon samples. This species has osteocytes in the vertebra with long cytoplasmic

processes that run through canaliculi in the bone. (ii) Some specimens were embedded in paraffin according to standard protocol. Ten-micrometre-thick sections were processed according to the method of Schmorl (1934) in order to search for bone canaliculi. Two procedures were employed for grinding. (iii) Undecalcified vertebrae were cut transversely in equal halves for grinding, and submerged in 100% acetone before air-drying. An Artech astera II 2s robot was used to slightly grind and polish the vertebrae on one end, which was glued to a microscope slide. The protruding end was then ground down to a specimen thickness of 30 μm before final polishing. A cover-slip was glued to the specimen using a mixture of SpeciFix resin and curing agent (Struers A/S, Ballerup, Denmark). (iv) Some undecalcified vertebrae were sawn into two halves and embedded in EpoFix resin mixed with EpoFix hardener in the proportions of 15 : 2. The polymerized specimens were ground with SiC-paper of increasing fineness, and subsequently polished with diamond spray to a thickness of 0.1–0.3 mm. All specimens were examined on an Olympus Vanox AHBT3 microscope (Olympus, Tokyo, Japan) employing both bright-field and differential interference contrast (DIC) optics. Digital micrographs were acquired with a ProgRes C14 camera (Jenoptik GmbH, Jena, Germany), and Adobe Photoshop CS (Adobe Systems, San Jose, CA, USA) was used for image processing.

Vertebrae 43 and 44 from 12 fish per group were used to measure osteocyte density (cells per mm^2 of bone) on semi-thin sections (2 μm) of methacrylate-embedded tissue from both lamellar (autocentrum) and cancellous compartments (arcocentrum). In non-exercised fish, 19.74 mm^2 of lamellar bone and 46.37 mm^2 of cancellous bone were analysed for the presence of osteocytes, while 36.6 mm^2 of autocentrum and 66.3 mm^2 of arcocentrum were analysed in the exercised group. A total of 9123 osteocytes were identified. Cell counts were analysed using CELL^P software (Olympus Soft Imaging Solutions GmbH, Hamburg, Germany).

For electron microscopy, salmon vertebrae and vertebrae from *Polypterus ornatipinnis* were fixed, decalcified, embedded in Epon, sectioned at 50 μm and studied in a Jeol 1011 transmission electron microscope. Samples of vertebrae from exercised and non-exercised salmon were processed for scanning electron microscopy as described in Nordvik et al. (2005), and studied in a Zeiss supra 55V field emission scanning electron microscope.

RNA isolation

Vertebrae 45 and 46 were used for RNA isolation. The vertebrae were cleansed of surrounding tissue (muscle/neural tube) before being flash frozen on liquid nitrogen. For RNA isolation, frozen vertebrae were cut into small pieces and then crushed. RNA was extracted using the FastRNA Pro Green kit (Qbiogene, CA, USA). RNA was DNAse treated using TURBO DNA-*free*^{TM} (Ambion, TX, USA) according to the manufacturer's recommendations. The amount and quality of RNA was assessed by means of a Nanodrop ND-1000 spectrophotometer (NanoDrop Technologies, Wilmington, DE, USA).

qPCR

Gene expression analysis was performed in order to assay gene expression differences in response to exercise. The following genes, all with properties related to bone matrix mineralization, were analysed: *alkaline phosphatase* (*alp*), *collagen type 1 alpha 2* (*col 1*), *insulin growth factor receptor* (*igf-1R*), *growth hormone receptor* (*ghr*), *bone* γ*-carboxyglutamic acid protein* (*bgp*) (synonym *osteocalcin*) *and insulin growth factor-I* (*igf-I*). All reactions were run on the 7900 HT Fast Real-Time PCR system. The conditions for PCR for all the reactions were 50 °C for 2 min followed by 95 °C for 10 min, and the reactions thereafter proceeded through 40 cycles of 95 °C for 15 s followed by 60 °C for 1 min. In all the experiments no-template controls were run together with the samples. The efficiency of targets in relation to reference gene, elongation factor 1α (Olsvik et al. 2005) was determined using a standard curve method together with a validation experiment (ABI User Bulletin #2 for ABI 7700 sequence detections system). In the validation experiment, 500, 250 and 125 ng RNA were used for cDNA synthesis, and the slope of log input amount of RNA vs. delta *C*t was < 0.1 between reference gene and target genes, which demonstrates that the efficiencies of target and reference genes were approximately equal. The methods and primers used have already been published: *alp*, *col I* (Wargelius et al. 2009); *igf-IR* and *ghr* (Wargelius et al. 2005), *bgp* (Krossøy et al. 2009) and *igf-I* (Nordgarden et al. 2006).

Calculations and statistical analysis

Specific growth rate (SGR) was calculated using: SGR body weight = $(e^G - 1) \times 100$, where $G = (\ln(X_2) - \ln(X_1))\ (t_2 - t_1)^{-1}$; X_2 and X_1 are the body weights at times t_2 and t_1. ANCOVA was employed to test whether the micro-CT parameters differed between the two groups. Differences in the mineral content and mechanical properties of the vertebral bone, in addition to fish weight, length and osteocyte density of the lamellar (autocentrum) and cancellous bone (arcocentrum) of the vertebrae were tested using nested ANOVAs followed by a Newman–Keuls test. A *P*-value < 0.05 was considered to be statistically significant. Q-Gene software application was used to quantify gene expression, and REST (Relative Expression Software Tool) for statistical analysis.

Results

Parallel somatic growth rate within normal range in the two groups

There was no significant difference in gain of weight ($\sim$ 2.5-fold) or length ($\sim$ 7 cm) between the non-exercise and exercise groups (Fig. 4a,b). The mean SGRs of 1.42 and 1.46, respectively, were within the normal range of somatic growth for farmed post-smolts (Handeland et al. 2003). This indicates that both groups had been exposed to an environment that promoted normal growth and development.

Increased vertebral BMC and improved stiffness

The vertebrae taken from the exercised group had a significantly higher stiffness than that of the non-exercise group (Fig. 5a). There were no group differences in yield load or resilience (data not shown). The bone mass measured as BMC was significantly higher in fish of the exercise group, with an increase of 5% (Fig. 5b).

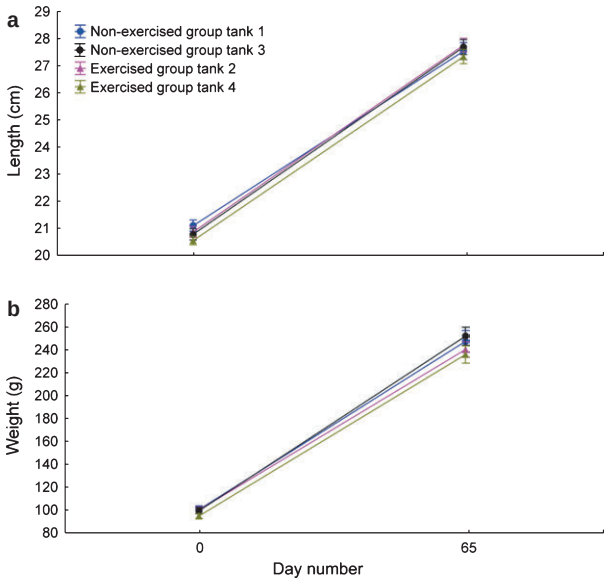

Fig. 4 Gain in length and weight in the exercised and non-exercised group during the experiment. (a) No significant differences in the increase in fish fork length between the two groups. (b) No significant differences in the weight increase between the two groups.

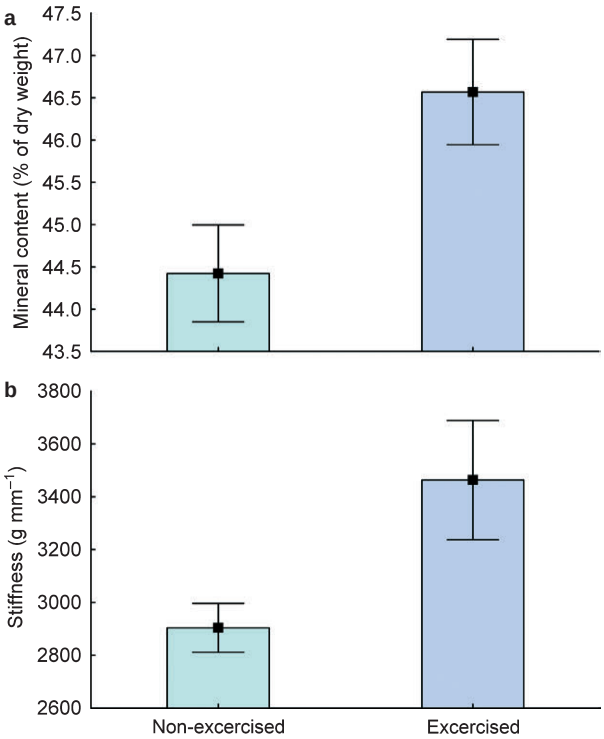

Fig. 5 Mineral content and stiffness of vertebrae. (a) Mineral content in the exercised and non-exercised group (mean values ± SEM). There was a significant difference between the groups. (b) Stiffness (g × mm^{-1}) of vertebrae in the exercised and non-exercised group was tested using a compression jig mounted in a servo-hydraulic machine (mean values ± SEM). For all vertebrae, there were significant differences between the exercised and non-exercised groups. [Corrections were introduced to the figure on 20 June 2011 after its first publication online in Wiley Online Library on 25 May 2011.]

Sustained vigorous swimming did not affect vertebral body architecture

No significant group differences in the length or diameter of the vertebrae were found. The three-dimensional morphometric parameters based on analysis of data obtained by micro-CT, employed to quantify the bone architecture, showed very similar values in the exercised and non-exercised groups. The micro-CT images enabled 'digital dissections' of the vertebral body to be made, and revealed that the longitudinal and transverse plates of the cancellous bone at this life-stage were continuous with the compact lamellar bone of the amphicoel in both the exercised and non-exercised groups.

The vertebral osteocytes do not form a functional communicating network

The open architecture of salmon vertebral bone requires osteoblasts to be located close to the cranial and caudal rims of the lamellar amphicoel. The osteoblasts on the cancellous bone are mainly located along the distal ends of the longitudinal and transverse bone plates (Figs 1a,b and 6a,b). This implies polarized secretion of osteoid in these regions, and the osteoid is deposited from the basal domain of the long cylindrical osteoblasts facing the bone matrix (Fig. 6b). The osteocytes do not appear to be recruited from these osteoblast groups, as the bone matrix below was virtually free of cells (Fig. 6a).

The osteocytes were spindle-shaped with the long axis parallel to the surrounding collagen fibres (Fig. 7a–c). The osteocyte nuclei were light-staining reflecting abundant euchromatin, thus indicating that these were active cells. Canaliculi or cytoplasmic extensions were not observed with any of the techniques employed (Fig 7a–c), including transmission electron microscopy (data not shown). In the control material from *Polypterus* the osteocytes had a well-developed network of cellular processes, which could be observed in both light and electron microscopy (Fig. 7d).

The osteocyte density of the compact lamellar bone of the amphicoel was significantly higher in the exercised than non-exercised group ($P = 0.006244$). The osteocyte density was ~ 20% higher at 35.4 ± 2.6 cells mm^{-2} in the exercised group than the 25.9 ± 1.7 cells mm^{-2} of the non-exercised fish. In the exercised group the highest osteocyte density was found in the external regions of the lamellar bone (Figs 6c and 9). The osteocytes may be recruited from small osteoblasts in this region (Fig. 6c). The lamellar bone in the rim region was almost devoid of osteocytes (Fig. 6a,b). In the cancellous bone osteocytes were more abundant, and no difference in density between the two groups was found (Fig. 6d), with 67.1 cells mm^{-2} in non-exercised and 68.3 cells mm^{-2} in exercised fish.

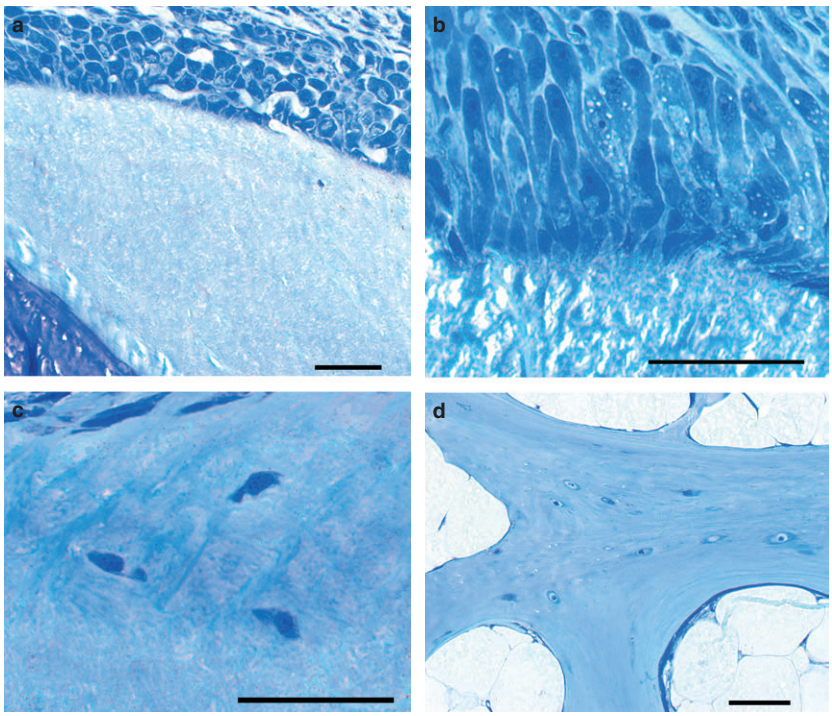

Fig. 6 Salmon vertebral osteoblasts and osteocytes. (a) The external rim of the autocentrum, with abundant osteoblasts and a nearly cell-free bone matrix. (b) Osteoblasts on the external rim of the autocentrum are club-shaped with a narrow base towards the osteoid. (c) Osteocytes in the preferred location in the autocentrum: in the vicinity of the attachment to the arcocentrum. (d) Osteocytes, relatively abundant, in the arcocentrum. Scale bar: 50 μm – valid for all figures.

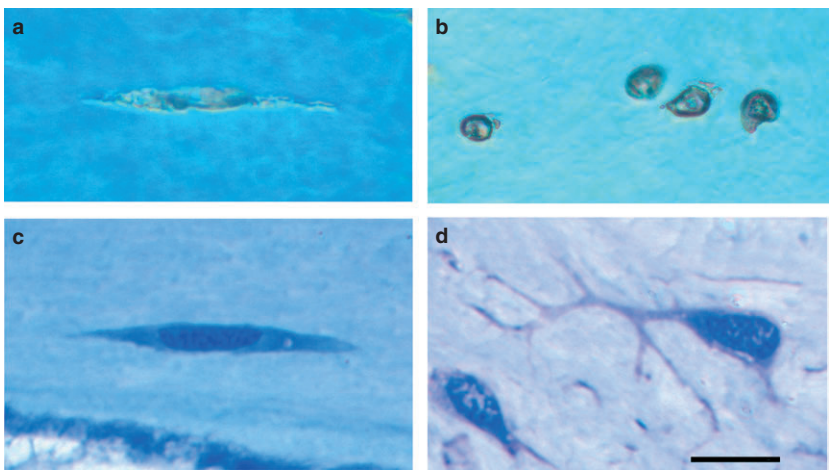

Fig. 7 Vertebral osteocytes. (a) Grinded specimen from salmon with osteocytes in longitudinal orientation. Note the absence of canaliculi. (b) Grinded specimen from salmon with osteocytes in transverse orientation. (c) Technovit section of longitudinally oriented salmon osteocytes. Notice the absence of dendritic osteocytic processes. (d) A representative Technovit control section from bichir, showing well-developed dendritic osteocytic processes. Scale bar: 10 μm – applies to all figures.

An extremely low density of multinuclear osteoclasts (0.1–0.3 cells mm^{-2}) and a few signs of bone resorption (Howship's lacunae) were found in the cancellous bone, with no differences being observed in the exercised and non-exercised groups.

Differences in gene expression

Both expression of *bgp* and *alp* mRNAs were significantly upregulated in the exercised fish ($P < 0.05$), while mRNA expression of *ghr*, *igf-I*, *igf-1R* and *col 1* was not affected by exercise (Fig. 8).

Discussion

Bone tissue is dynamic. In mammals, bone adapts to mechanical stresses largely by altering its size and shape. It has been suggested that strains produced in response to mechanical loading throughout the bone matrix are detected by communicating osteocytes that transduce signals, orchestrating osteoblast and osteoclast activity in order to fine-tune properties to functional requirements (Yeh et al. 1993). An intriguing question is how teleost osteocytic vertebral bone responds to increased load caused by sustained strenuous exercise within the normal physiological

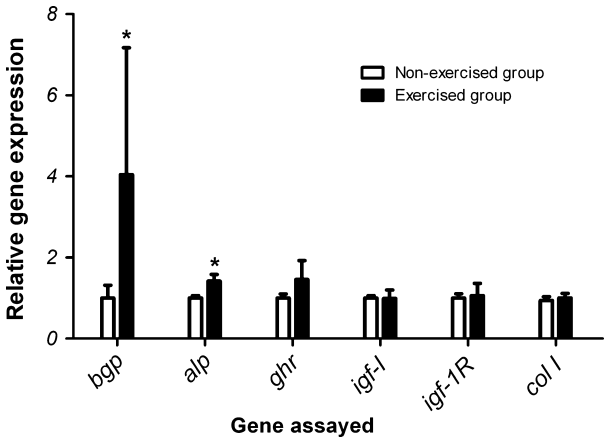

Fig. 8 Gene expression of *osteocalcin* (*bgp*), *alkaline phosphatase* (*alp*), *growth hormone receptor* (*ghr*), *insulin growth factor I* (*igf-I*), *insulin growth factor I receptor* (*igf-1R*) and *collagen type 1 alpha 2* (*col I*) in vertebral bone of exercised (black bars) and non-exercised (white bars) fish. The genes are listed on the *x*-axis, while the *y*-axis indicates the relative abundance of the transcripts in relation to the normalization factor *elongation factor1α*. Data are presented as means ± SEM Significant gene expression differences between the two groups are indicated by an asterisk (*$P < 0.05$).

range and, furthermore, whether it possesses the ability to sense changes in the mechanical load, similar to that of mammalian bone. We show here in Atlantic salmon vertebrae that fast sustained swimming affects bone matrix properties by increasing the matrix mineral content without a change in bone accretion. Furthermore, the osteocytes of vertebral bone do not appear to form a functional communicating syncytium network. In addition, the osteocyte density in the exercised fish increased significantly in the compact lamellar bone of the amphicoel, but not in the cancellous bone. Mechanical stimulation in this layer may thus activate osteoblasts and tune the genetic pathways that regulate the secretion of proteins that determine the process of mineral formation, in this way continuously adjusting bone properties to functional demands.

Increased incorporation of mineral content into osteoid in response to load

In mammals, loading imposed by exercise under gravitational stress initiates a cascade of complex physiological events that stimulates bone formation and strengthens the skeleton, thus increasing bone mineral density (BMD; Turner, 2006; Wallace et al. 2007; Warden et al. 2007). Even a small increase in mineral density can improve bone strength significantly (see review by Turner, 2006). There is considerable evidence that when load increases, not only is bone added at a greater rate with increased loading frequency, but the loading force required to stimulate bone growth also diminishes, a phenomenon that cannot be fully explained by an increase in bone mass and architectural modification (Wallace et al. 2007; Kohn et al. 2009). The mechanical properties of bone also depend on matrix composition and structure – both mineral composition and content and its collagen quality and three-dimensional arrangement may have an impact. Just how collagen cross-linking affects the mineralization of bone is an intriguing question, but further studies are required to establish whether the patterns of cross-links formed play a causal or merely a permissive role. All in all, modification of the collagen phase of the vertebral bone matrix, either through change of arrangement or increased cross-binding, may contribute less than the observed increase in mineral content to the improvement of stiffness in response to loading, as matrix mineral content in salmon bone correlates well with stiffness (Fjelldal et al. 2006, 2009). The fact that *col I* transcription did not increase in the exercised group in our study suggests that there is no marked increase in extracellular matrix collagens, which is consistent with the observation that there are no structural alterations in response to the exercise. However, *col I* expression in salmon vertebrae may not necessarily reflect the incorporation rate of collagen I into matrix (Wargelius et al. 2009), as has also been observed in bovine cortical bone (Garnero et al. 2006).

Our study indicates that the morphogenetic pathways that dictate the shape and volume of the vertebral body are not changed by exercise; in extension, the total volume of secreted osteoid thus seems to be independent of mechanical loading. However, matrix quality is modified by an increase in mineral content. This observation is in agreement with an exercise study of rainbow trout throughout their lifecycle (Deschamps et al. 2009), which showed that increasing the swimming speed enhanced vertebral bone mineralization and reduced the appearance of fused vertebrae. Two-dimensional measurements revealed a decrease in vertebral area, which is different from our results. The divergence may be due to species differences in vertebral morphogenesis, the developmental stage studied, or effects caused by the different methods employed to quantify vertebral bone.

The increased bone mass found in the exercised fish in our study may be dependent on the amount of non-collagenous proteins secreted, including the proteins that modulate mineral incorporation. All the components needed to initiate the mineralization process and maintain mineral accretion are inherent properties of the bone matrix itself. The higher level of mRNAs for both *bgp* and *alp* in the exercised group that encode proteins detected during osteogenesis in salmon (Krossøy et al. 2009; Wargelius et al. 2009) indicates that these genes may be involved in the mineralization process. In mammals, it has been indicated that *alp* provides a high PO_4 concentration at the osteoblast cell surface during the formation of HA crystals (Noda et al. 1984; Rawadi et al. 2003; Ryan et al.

2008), while *bgp* may coordinate calcium-binding properties that may be important in the regulation of bone growth (Dimuzio et al. 1983; Boskey et al. 1998). The main effect of exercise on bone physiology in teleosts may be regulation of the amount of non-collagenous proteins secreted, for instance through a mechanocoupling to gene transcription.

Which part of the vertebral body in the exercised fish is enforced by a higher mineral content?

The increase in BMC found in the exercised group is probably concentrated in the external region of the vertebral body, where bone formed during the experiment (Fig. 9). On the other hand, it cannot be completely ruled out that mineral content may also have increased in the pre-existing bone matrix at the core, similar to that found in bone of grown mice subjected to exercise (Kohn et al. 2009). It was found that the sole effect was an increase in mineral content in non-remodelling intercortical bone. The teleost vertebra is an open structure (Fig. 1a,b) with no outer delimiting cortical bone, such as is found in mammals. This facilitates unlimited outward growth, where the amphicoelous cones extend at the rims, resulting in an increase in length and diameter, and the longitudinal and transverse supportive plates increase in area through accretion of bone at their distal ends; concurrently, the number of plates increases through branching. Through this morphogenesis bone tissue is progressively older towards the middle of the vertebral body, while fresh bone continuously accrues at the periphery (Fig. 9). In other words, if the increase in mineral content in the exercised group is limited to the bone formed during the experiment, it will be confined to the peripheral areas of the vertebral body that include the rims of the compact cones of the amphicoel and the reinforcing struts and trusses of the cancellous bone. These regions provide the greatest resistance to bending and torsion (Ruff & Hayes, 1988). Osteogenesis may in this way be directed to the regions where it is most needed for improving bone strength. How these complex vertebral structures are related to specific mechanical properties remains to be investigated.

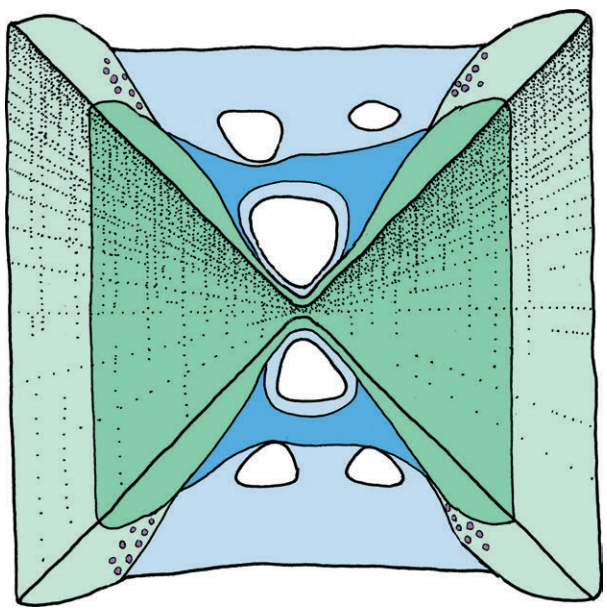

Fig. 9 Schematic illustration of a median section through a vertebra. The vertebral body consists of the lamellar bone (the autocentrum, in dark blue) and the cancellous bone (arcocentrum, in dark green), as it was at the start of the experiment. During the experiment, new bone was formed in both compartments, here shown in light blue and light green. The region with the highest increase in osteocyte density in the exercised group is indicated by violet circles and was found in the newly formed bone of the autocentrum, close to the attachment to the arcocentral struts.

Why increase the bone matrix mineral content and not alter the architecture?

The interactions among mass, shape and matrix quality that determine the properties of bone are not well understood. All ray-finned fish are denser than water, so they tend to sink; their negative buoyancy is influenced by the mineral content of their skeleton and, compared with tetrapods, their BMC is significantly lower (Meunier, 2002). Furthermore, the skeleton makes up a smaller proportion of the total body mass (Reynolds & Karlotski, 1977). The increase in BMC found in the exercised group may represent a compromise in phenotypic plasticity that offers optimal mechanical competence without an undue increase in bone weight, and therefore body density, which would contribute to negative buoyancy and the need for a greater swimbladder volume. Even a small addition of BMD (5–8%) in mammals as a result of increased mechanical loading may improve bone strength by more than 60% (Turner, 2006). In salmon, the architecture of the cancellous bone allows a considerable amount of fat to be deposited between the plates. This may counteract the effect of an increase in BMC on body density.

How do the osteocytes maintain bone structural integrity and strength?

The significance of the increased osteocyte density in the lamellar bone of the autocentrum in the exercised group and not in the cancellous part is difficult to elaborate. The main increase in osteocyte density was found in the outer layer of the lamellar bone of the autocentrum, and they had probably been recruited from osteoblasts located on the surface of the bone in this region. Here, the osteoblasts were smaller than those at the rim of the autocentrum, which may influence the frequency of osteoblast-to-osteocyte transformation, making the osteoblast more prone to

incorporation into the matrix. This is supported by the fact that the lamellar bone at the rim is practically devoid of osteocytes.

The increase in osteocyte density may reflect the possibility that osteoblasts in the adjacent region were stimulated by the sustained exercise, possibly increasing the osteoblast-to-osteocyte transformation and the mineral content, and thus contributing to the increased vertebral stiffness. The difference in response in the lamellar and cancellous compartments may reflect the fact that the osteoblasts of the arcocentrum and autocentrum in salmon, which deposit bone with a different matrix structure and cellularity (lamellar and cancellous), also display functional differences at the molecular level.

How the increase in osteocyte density affects the lamellar bone of the autocentrum is not clear. *In situ* osteocytes are thought to be subject to one of two fates: death by apoptosis or resorption by osteoclasts (Parfitt, 2002). Our results indicate that bone resorption is low in the post-smolt life-stage in both groups. We cannot, however, rule out the possibility that the observed increase in osteocyte density may be a result of a reduced level of apoptosis.

Are salmon vertebral osteocytes mechanosensory cells?

The osteocyte density in salmon vertebral bone is far lower than that of tetrapods (Mullender et al. 1996; Hall, 2005; Nordvik et al. 2005; Witten & Huysseune, 2009). As pointed out, tetrapod osteocytes possess cell processes that lie within canaliculi, and this is believed to be the case also in some teleost osteocytic bone types (Stéphan, 1900; Meunier & Huysseune, 1992; Huysseune, 2000; Meunier, 2002; Witten & Hall, 2002; Witten & Huysseune, 2009). However, as we show, the osteocyte density of salmon vertebral bone is so low and the osteocytes so far apart from each other and from the surface cells that a network of interconnections among them is highly unlikely. This being the case, the response to mechanical loading occurs in the absence of an osteocytic network, thus precluding the mammalian type of mechanosensing and indicating the existence of a different mechanotransduction mechanism. However, salmon vertebral osteocytes may produce chemical messengers. If so, the effect will depend on diffusion, which is determined by the same physical laws in all animals.

The most obvious mechanosensory cell candidates in salmon are osteoblasts or bone-lining cells on the bone surface, which would imply that signal detection and response are co-localized. This type of mechanosensing system is supported by the fact that mammalian osteoblasts and osteocytes *in vitro* are sensitive to mechanical load (Vatsa et al. 2006), and that mammalian odontoblasts seem to have a certain sensory capacity (Magloire et al. 2004; Allard et al. 2006). These aspects challenge our understanding of the mechanosensing system in teleost bone.

Acknowledgements

This project was financed by the Research Council of Norway (Project no. 164780/S40). Skilful technical assistance was provided by Teresa Cieplinska and Nina Ellingsen. We are also indebted to the staff of the Institute of Marine Research at Matre for laboratory assistance, and for rearing the fish.

References

Allard B, Magloire H, Couble ML, et al. (2006) Voltage-gated sodium channels confer excitability to human odontoblasts. Possible role in tooth pain transmission. *J Biol Chem* **281**, 29 002–29 010.

Bonewald LF (2005) Generation and function of osteocyte dendritic processes. *J Musculoskelet Neuronal Interact* **5**, 321–324.

Bonewald LF, Johnson ML (2008) Osteocytes, mechanosensing and Wnt signaling. *Bone* **42**, 606–615.

Boskey AL, Gadeleta S, Gundberg C, et al. (1998) Fourier transform infrared microspectroscopic analysis of bones of osteocalcin-deficient mice provides insight into the function of osteocalcin. *Bone* **23**, 187–196.

Burr DB (2002) The contribution of the organic matrix to bone's material properties. *Bone* **31**, 8–11.

Carter DR, van der Meulen MC, Beaupre GS (1996) Mechanical factors in bone growth and development. *Bone* **18**(1 Suppl), S5–S10.

Coughlin DJ, Spiecker A, Schiavi JM (2004) Red muscle recruitment during steady swimming correlates with rostral-caudal patterns of power production in trout. *Comp Biochem Physiol Part A* **137**, 151–160.

Cowin SC, Moss-Salentijn L, Moss ML (1991) Candidates for the mechanosensory system in bone. *J Biomed Eng* **113**, 191–197.

Currey JD (1984) Can strains give ad information for adaptive bone remodeling. *Calcif Tissue Int* **36**, S118–S119.

Currey JD (2003) The many adaptations of bone. *J Biomech* **36**, 1487–1495.

Deschamps M-H, Labbé L, Baloche S, et al. (2009) Sustained exercise improves vertebral histomorphometry and modulates hormonal levels in rainbow trout. *Aquaculture* **296**, 337–346.

Dimuzio MT, Bhown M, Butler WT (1983) The biosynthesis of dentin γ-carbonxyglutamic acid-containing protein by rat incisor odontoblasts in organ culture. *Biochem J* **216**, 249–257.

Fiaz AW, van Leeuwen JL, Kranenbarg S (2010) Phenotypic plasticity and mechano-transduction in the teleost skeleton. *J Appl Ichthyol* **26**, 289–293.

Fjelldal PG, Grotmol S, Kryvi H, et al. (2004) Pinealectomy induces malformations of the spine and reduces the mechanical strength of the vertebrae in Atlantic salmon *Salmo salar*. *J Pineal Res* **36**, 1–8.

Fjelldal PG, Nordgarden U, Berg A, et al. (2005) Vertebrae of the trunk and tail display different growth rates in response to photoperiod in Atlantic salmon, *Salmo salar* L., post-smolts. *Aquaculture* **250**, 516–524.

Fjelldal PG, Lock E-J, Grotmol S, et al. (2006) Impact of smolt production strategy on vertebral growth and mineralisation

during smoltification and the early seawater phase in Atlantic salmon (*Salmo salar* L.). *Aquaculture* **261**, 715–728.

Fjelldal PG, Hansen T, Breck O, et al. (2009) Supplementation of dietary minerals during the early seawater phase increases vertebral strength and reduces the prevalence of vertebral deformities in fast-growing under-yearling Atlantic salmon (*Salmo salar* L.) smolt. *Aquac Nutr* **15**, 366–378.

Garnero P, Borel O, Gineyts E, et al. (2006) Extracellular posttranslational modifications of collagen are major determinants of biomechanical properties of fetal bovine cortical bone. *Bone* **38**, 300–309.

Hall BK (2005) *Bones and Cartilage: Developmental and Evolutionary Skeletal Biology*. London: Elsevier/Academic Press.

Handeland SO, Björnson BT, Arnesen AM, et al. (2003) Seawater adaptation and growth of post-smolt Atlantic salmon (*Salmo salar*) of wild and farmed strains. *Aquaculture* **220**, 367–384.

Huang TH, Lin SC, Chang FL, et al. (2003) Effects of different exercise modes on mineralization, structure, and biomechanical properties of growing bone. *J Appl Physiol* **95**, 300–307.

Hughes DR, Bassett JR, Moffat LA (1994) Histological identification of osteocytes in the allegedly acellular bone of the sea breams *Acanthopagurus australis*, *Pagrus auratus* and *Rhabdosargus sarba* (Sparidae, Perciformes, Teleostei). *Anat Embryol* **190**, 163–179.

Huysseune A (2000) Skeletal system. In: *The Laboratory Fish* (ed. Ostrander G), pp. 307–317. London: Academic Press.

Huysseune A, Sire J-Y, Meunier FJ (1994) Comparative study of lower pharyngeal jaw structure in two phenotypes of *Astatoreochromis alluaudi* (Teleostei:Cichlidae). *J Morphol* **221**, 25–43.

Kohn DH, Sahar ND, Wallace JM, et al. (2009) Exercise alters mineral and matrix composition in the absence of adding new bone. *Cells Tissues Organs* **189**, 33–37.

Kölliker A (1859) On the different types in the microscopic structure of the skeleton of osseous fishes. *Proc R Soc Lond* **9**, 65–68.

Krossøy C, Ørnsrud R, Wargelius A (2009) Differential gene expression of *bgp* and *mgp* in trabecular and compact bone of Atlantic salmon (*Salmo salar* L.) vertebrae. *J Anat* **215**, 663–672.

Liao JC (2007) A review of fish swimming mechanics and behaviour in altered flow. *Philos Trans R Soc B* **362**, 1973–1993.

Lynne R, Parenti FLS (2008) The phylogenetic significance of bone types in euteleost fishes. *Zool J Linn Soc* **87**, 37–51.

Magloire H, Couble ML, Romeas A, et al. (2004) Odontoblast primary cilia: facts and hypotheses. *Cell Biol Int* **28**, 93–99.

Meunier FJ (2002) Skeleton. In: *Manual of Fish Sclerochronology* (eds Panfili J, de Pontual H, Troadec H, Wright PJ), pp. 65–88. Brest, France: Ifremer-IRD coedition.

Meunier FJ, Huysseune A (1992) The concept of bone tissue in Osteichthyes. *Neth J Zool* **42**, 445–458.

Meunier FJ, Ramzu MY (2006) Functional regionalisation of the vertebral axis related to the swimming mode in the Teleostei. *C R Palevol* **5**, 499–507.

Meunier FJ, Sire J-Y (1981) Sur la structure et la minéralisation des écailles de germon, *Thunnus alalunga* (Téleostéen, Perciforme, Thunnidae). *Bull Soc Zool Fr* **106**, 327–336.

Moss ML (1961) Studies of the acellular bone in teleost fish I. Morphological and systematic variations. *Acta Anat* **46**, 343–362.

Moss ML (1965) Studies of the acellular bone of teleost fish V. Histology and mineral homeostasis of fresh-water species. *Acta Anat* **60**, 262–276.

Mullender MG, Huiskes R (1995) Osteocytes and bone lining cells: which are the best candidates for mechano-sensors in cancellous bone? *Bone* **20**, 527–532.

Mullender MG, Huiskes R, Versleyen H, et al. (1996) Osteocyte density and histomorphometric parameters in cancellous bone of the proximal femur in five mammalian species. *J Orthop Res* **14**, 972–979.

Noda M, Majeska R, Rodan GA (1984) Relationship between cell proliferation, cell density and alkaline phosphatase expression in an osteoblastic osteosarcoma cell line. *Calcif Tissue Int* **36**, 467.

Nordgarden U, Fjelldal PG, Hansen T, et al. (2006) Growth hormone and insulin-like growth factor-I act together and independently when regulating growth in vertebral and muscle tissue of Atlantic salmon postsmolts. *Gen Comp Endocrinol* **149**, 253–260.

Nordvik K, Grotmol S, Kryvi H, et al. (2005) The salmon vertebral body develops through mineralization of two preformed tissues that are encompassed by two layers of bone. *J Anat* **206**, 103–114.

Notomi T, Okimoto N, Okazaki Y, et al. (2001) Effects of tower climbing exercise on bone mass, strength, and turnover in growing rats. *J Bone Miner Res* **16**, 166–174.

Økland F, Thorstad EB, Finstad B, et al. (2006) Swimming speeds and orientation of wild Atlantic salmon post-smolts during the first stage of the marine migration. *Fish Manag Ecol* **13**, 271–274.

Olsvik PA, Lie KK, Jordal AEO, et al. (2005) Evaluation of potential reference genes in real-time RT-PCR studies of Atlantic salmon. *BMC Mol Biol* **6**, 1–9.

Palumbo C, Palazzini S, Zappe D, et al. (1990) Osteocyte differentiation in the tibia of newborn rabbits: an ultrastructural study of the formation of cytoplasmic processes. *Acta Anat* **137**, 350–358.

Parenti LR (1986) The phylogenetic significance of bone types in euteleost fishes. *Zool J Linn Soc* **87**, 37–51.

Parfitt AM (2002) Life history of osteocytes: relationship to bone age, bone remodelling and bone fragility. *J Musculoskelet Neuronal Interact* **2**, 499–500.

Rawadi G, Vayssiere B, Dunn F, et al. (2003) BMP-2 controls alkaline phosphatase expression and osteoblasts mineralization by a Wnt autocrine loop. *J Bone Miner Res* **18**, 1842–1853.

Reynolds WW, Karlotski WJ (1977) Allometric relationship of skeleton weight to body-weight in teleost fishes – preliminary comparison with birds and mammals. *Copeia* **1**, 160–163.

Robling AG, Turner CH (2009) Mechanical signalling for bone modelling and remodelling. *Crit Rev Eukaryot Gene Expr* **19**, 319–338.

Ruff CB, Hayes WC (1988) Sex differences in age-related remodelling of the femur and tibia. *J Orthop Res* **6**, 886–896.

Ryan SW, Truscott J, Simpson M, et al. (2008) Phosphate, alkaline phosphatase and bone mineralization in preterm neonates. *Acta Paediatr* **82**, 518–521.

Schmorl G (1934) *Die Pathologisch-Histologischen Untersuchungsmethoden*, pp. 259. Berlin: Vogel.

Stéphan P (1900) Recherches histologiques sur la structure du tissu osseux des poissons. *Bull Sci Fr Belg* **33**, 281–429.

Tang J, Wardle CS (1992) Power output of two sizes of Atlantic salmon (*Salmo salar*) at their maximum sustained swimming speeds. *J Exp Biol* **166**, 33–46.

Timlin JA, Carden A, Morris MD, et al. (2000) Raman spectroscopic imaging markers for fatigue-related microdamage in bovine bone. *Anal Chem* **72**, 2229–2236.

Turner CH (2006) Bone strength: current concepts. *Ann NY Acad Sci* **1068**, 429–446.

Turner CH, Robling AG (2005) Mechanisms by which exercise improves bone strength. [Review]. *J Bone Miner Metab* **23**, S16–S22.

Turner CH, Warden SJ, Bellido T, et al. (2009) Mechanobiology of the skeleton. *Sci Signal* **2**, pt3.

Vatsa A, Mizuno D, Smit TH, et al. (2006) Bio imaging of intracellular NO production in single bone cells after mechanical stimulation. *J Bone Miner Res* **21**, 1722–1728.

Wallace JM, Rajachar RM, Allen MR, et al. (2007) Exercise-induced changes in the cortical bone of growing mice are bone- and gender-specific. *Bone* **40**, 1120–1127.

Warden SJ, Fuchs RK, Castillo AB, et al. (2007) Exercise when young provides lifelong benefits to bone structure and strength. *J Bone Miner Res* **22**, 251–259.

Wardle CS, Videler JJ, Altringham JD (1995) Tuning in to fish swimming waves: body form, swimming mode and muscle function. *J Exp Biol* **198**, 1629–1636.

Wargelius A, Fjelldal PG, Benedet S, et al. (2005) A peak in gh-receptor expression is associated with growth activation in Atlantic salmon vertebrae, while upregulation of *igf*-I receptor expression is related to increased bone density. *Gen Comp Endocrinol* **142**, 163–168.

Wargelius A, Fjelldal PG, Nordgarden U, et al. (2009) Continuous light affects mineralization and delays osteoid incorporation in vertebral bone of Atlantic salmon (*Salmo salar* L.). *J Exp Biol* **212**, 656–661.

Weiss RE, Watabe N (1979) Studies of the biology of fish bone. III. Ultrastructure of osteogenesis and resorption in osteocytic (cellular) and anosteocytic (acellular) bones. *Calcif Tissue Int* **28**, 43–56.

Witten PE, Hall BK (2002) Differentiation and growth of kype skeletal tissues in anadromous male Atlantic salmon (*Salmo salar*). *Int J Dev Biol* **46**, 719–730.

Witten PE, Huysseune A (2009) A comparative view on mechanisms and functions of skeletal remodelling in teleost fish, with special emphasis on osteoclasts and their function. *Biol Rev* **84**, 315–346.

Yeh JK, Liu CC, Aloia JF (1993) Effects of exercise and immobilization on bone formation and resorption in young rats. *Am J Physiol* **264**, E182–E189.

Zylberberg L, Geraudie J, Meunier F, et al. (1992) Biomineralization in the integumental skeleton of the living lower vertebrates. In :*Bone* (ed. Hall BK), pp. 171–224. Boca Raton, Ann Arbor: CRC Press.